Models of Rotary Vacuum Drum and Disc Filters for Flocculated Suspensions

Anthony D. Stickland
Particulate Fluids Processing Centre, Dept. of Chemical and Biomolecular Engineering, The University of Melbourne, Victoria 3010, Australia

Lee R. White
School of Mathematics and Statistics, University of South Australia, Mawson Lakes, South Australia 5095, Australia

Peter J. Scales
Particulate Fluids Processing Centre, Dept. of Chemical and Biomolecular Engineering, The University of Melbourne, Victoria 3010, Australia

DOI 10.1002/aic.12310
Published online June 25, 2010 in Wiley Online Library (wileyonlinelibrary.com).

Models for rotary drum and disc filtration of compressible suspensions are developed using one-dimensional compressional rheology theory. The models account for cake formation while the drum or disc is submerged in the feed slurry, saturated cake consolidation upon surfacing due to capillary pressure, and cake desaturation. Desaturation does not occur for vacuum pressures below a critical value given by the material properties, or is incomplete if the formation and consolidation angles are too large. The disc filter model is formulated by applying the drum filter solutions to concentric annuli. The effect of different operating parameters such as submerged depth, rotational rate, slurry concentration, and vacuum pressure are investigated. The throughput varies linearly or quadratically with the drum or disc radius respectively, proportionally with the square-root of the angular rotational speed and linearly with the submerged angle. The angles for cake consolidation and desaturation are independent of the rotational rate. © 2010 American Institute of Chemical Engineers *AIChE J,* 57: 951–961, 2011

Keywords: compressional rheology, solid/liquid separations, rotary vacuum filters, mathematical modeling

Introduction

Continuous rotary vacuum drum and disc filters are used in many industries to perform suspension dewatering. Models of these devices allow prediction of their performance and optimization of the operating conditions, and provide a basis for design. As illustrated in Figure 1, a drum filter essentially consists of a rotating cylindrical filter membrane (radius r_d, length L, angular speed ω) that is partly submerged (subtending angle θ_F) in a slurry bath (at solids volume fraction ϕ_0). The inside of the drum is held at pressure $p_0 - \Delta p$, where p_0 is the ambient pressure. The differential pressure, Δp, causes filter cake to form on the membrane while the drum is submerged, followed by cake consolidation (θ_C) and desaturation (θ_D). A knife or blade is positioned (θ_k) to scrape the product from the membrane. The related disc filter consists of a bank of M porous rotating vertical discs (radius r_d, angular speed ω) submerged by angle θ_F in slurry of volume fraction ϕ_0, where filter cake is deposited on the exterior surfaces (see Figure 2—the

Correspondence concerning this article should be addressed to A. D. Stickland at stad@unimelb.edu.au.

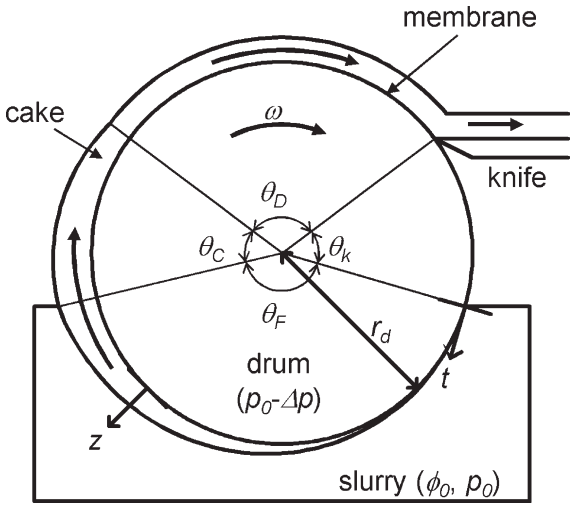

Figure 1. Schematic of vacuum drum filter.

subscripts in Figure 2 are described later). The differential pressure between the internal and external surfaces of the disc is Δp. Rotating vacuum filters may also include cake washing and air blowing features, but these are not considered here.

Models for the prediction of the performance of rotary vacuum filters have developed using incompressible descriptions of material behavior.[1–5] Although they do include the analysis of important issues such as membrane resistance, drum/disc partitioning and hydrostatic head, they have limited use for compressible materials such as flocculated suspensions. Buscall and White[6] developed a phenomenological model for the dewatering of compressible materials in which the solid phase forms a continuous network of volume fraction ϕ that has a physical strength called the compressive yield stress, $p_y(\phi)$. The network yields if $p_y(\phi)$ is exceeded and the rate at which fluid exudes is determined by the solid–liquid drag or hindered settling function, $R(\phi)$. This description has been used to model saturated dewatering processes such as dead-end pressure filtration,[7] batch thickening[8] and batch centrifugation,[9] for example.

During dewatering by air displacement or vacuum pressure, particulate networks also exhibit a capillary pressure, p_{cap}, at the air–liquid interface due to surface tension and the curvature of the particles. As with p_y, the maximum capillary pressure, p_{cap}^{max}, is also a function of ϕ.[10] The two functions intercept at the critical concentration, ϕ_{cap}. The cake will consolidate if $p_y(\phi) < \Delta p \leq p_{cap}^{max}(\phi)$ and desaturate if $\Delta p > p_{cap}^{max}(\phi)$. This approach was used to model the consolidation and desaturation of compressible materials due to drying[11,12] and centrifugal filtration,[13] and is the basis for a model of one-dimensional vacuum filtration.[14] Incompressible vacuum filtration models[15–17] describe only the drainage of interstitial fluid and fail to account for consolidation.

This work details the formulation of vacuum drum and disc filter models for compressible materials. The conservation of mass and momentum equations are given, boundary conditions outlined and solutions presented for cake formation, consolidation, and desaturation. The drum filter model is extended for use with vacuum disc filters by dividing the disc into concentric annuli and applying the drum filter model to individual pieces (see Figure 2). Model results are presented to illustrate the effect of operating parameters θ_F, ω, Δp, and ϕ_0.

Theory

The vacuum filtration model presented here assumes that the cake is thin enough to ignore the macroscopic radial geometry of the problem, such that the cake formation, consolidation, and desaturation processes are regarded as one-dimensional from the surface of the drum or disc using a normal coordinate, z, measured from the membrane surface. The angular position is given by t, where $t = 0$ is the position where the membrane is first submerged in the bath. t is simply the ratio of the arc length and the angular velocity at a particular position:

$$t = \frac{\theta}{\omega} \tag{1}$$

Therefore, θ_F, θ_C, θ_D, and θ_k map to $t_F = \theta_F/\omega$, $t_C = (\theta_F + \theta_C)/\omega$, $t_D = (\theta_F + \theta_C + \theta_D)/\omega$, and $t_k = (2\pi - \theta_k)/\omega$, respectively.

Solid–liquid separation

The compressional rheology model of suspension dewatering[6,18] balances the hydrodynamic, hydrostatic, network pressure, and acceleration forces acting upon a volume element of suspension. Ignoring gravity, one form of the transient conservation of momentum equations for the solid and liquid phases in one-dimension (z) is given by Eqs. 2 and 3:

$$\frac{\phi}{1-\phi} R(\phi)(u_s - u_l) - \frac{\partial p_s}{\partial z} = 0 \tag{2}$$

$$\frac{\partial p_l}{\partial z} + \frac{\partial p_s}{\partial z} = 0 \tag{3}$$

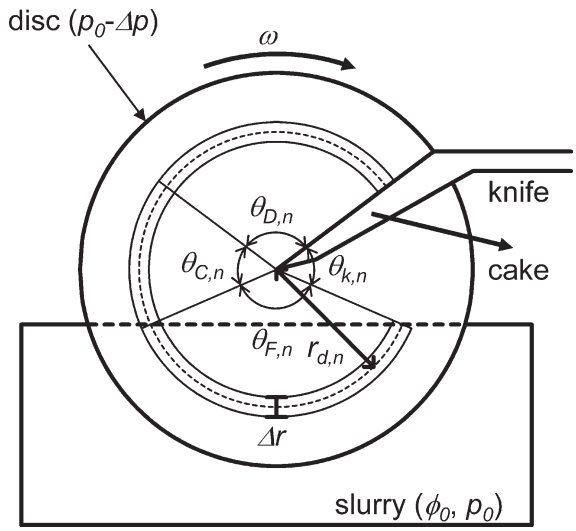

Figure 2. Schematic of vacuum disc filter.

$u_s - u_l$ is the local velocity of the solids relative to the liquid, and p_s and p_l are the local solid and liquid pressures. The conservation of mass equations for the two phases (assuming incompressibility of the individual phases) are given by Eqs. 4 and 5:

$$\frac{\partial \phi}{\partial t} = \frac{\partial (\phi u_s)}{\partial z} \tag{4}$$

$$\frac{\partial (1-\phi)}{\partial t} = \frac{\partial ((1-\phi) u_l)}{\partial z} \tag{5}$$

Adding Eqs. 4 and 5 and integrating gives the conservation of suspension:

$$\phi u_s + (1-\phi) u_l = s(t) \tag{6}$$

$s(t)$ is the bulk flow, which is equal to the specific flowrate of filtrate, dv/dt (where v is the specific volume of filtrate at time t). Substituting Eq. 6 into Eq. 2 gives:

$$\frac{\phi}{(1-\phi)^2} R(\phi)(u_s - s) - \frac{\partial p_s}{\partial z} = 0 \tag{7}$$

Eliminating ϕu_s from Eqs. 4 and 7 gives

$$\frac{\partial \phi}{\partial t} = \frac{\partial}{\partial z}\left[\frac{(1-\phi)^2}{R(\phi)} \frac{\partial p_s}{\partial z} + \phi s\right] \tag{8}$$

If the drainage of the suspending fluid is rate-determining rather than the breaking and/or reformation of interparticle bonds, then $p_s \le p_y(\phi)$.[6,19] The network collapses only when p_s exceeds $p_y(\phi)$ and is then equal to $p_y(\phi)$. Substituting $p_y(\phi) = p_s$ into Eq. 8 gives the governing equation for one-dimensional pressure filtration[18]:

$$\frac{\partial \phi}{\partial t} = \frac{\partial}{\partial z}\left[D(\phi) \frac{\partial \phi}{\partial z} + \phi s\right] \tag{9}$$

$D(\phi)$ is the solids diffusivity and is defined as:

$$D(\phi) = \frac{(1-\phi)^2}{R(\phi)} \frac{dp_y(\phi)}{d\phi} \tag{10}$$

Cake formation

The feed slurry is assumed to be well-mixed, such that there is no sedimentation in the slurry bath and the concentration is constant. The initial conditions for the problem are:

$$\begin{aligned} \phi(z,0) &= \phi_0 \\ v(0) &= 0 \\ z_c(0) &= 0 \end{aligned} \tag{11}$$

$z_c(t)$ is the cake height. The assumptions are made that $\phi_0 < \phi_g$ and that any material that is in the cake stays in the cake as the drum rotates out of the slurry bath. A model for $\phi_0 \ge \phi_g$ would require a rheological model of the film-splitting process, combining the shear and compressional behavior of the network as the cake is lifted from the bath and slumps back into the bath. This is beyond the scope of this work.

There is no network above the cake; therefore the top of the cake at z_c is at the gel point, ϕ_g (the concentration at which a network forms, $p_y(\phi_g) = 0$):

$$\phi(z_c, t) = \phi_g \tag{12}$$

Material above the cake ($z > z_c$) remains at ϕ_0. The concentration gradient at z_c is given by integrating the solids conservation (Eq. 4) across the discontinuity at $z_c(t)$ and rearranging:

$$\left.\frac{\partial \phi}{\partial z}\right|_{z_c} = -\frac{\phi_g - \phi_0}{D_g}\left(\frac{dz_c}{dt} + s\right) \tag{13}$$

D_g is $D(\phi_g)$.

If it is assumed that the membrane resistance is negligible compared with the cake resistance[20] and that the hydrostatic head is small compared with the vacuum pressure (that is, either filtrate remains in the drum, the slurry is not deep or the vacuum pressure is large, $\Delta p \gg \rho_l g r_d (1 - \cos(\theta_F/2))$, then the boundary condition at the membrane surface ($z = 0$) is simply that p_s is equal to the differential pressure, Δp. As $p_s = p_y(\phi)$, the concentration at the membrane is constant:

$$\phi(0, t) = \phi_\infty \tag{14}$$

ϕ_∞ is the equilibrium solids volume fraction and is defined by $p_y(\phi_\infty) = \Delta p$. Significant membrane resistance can be incorporated[7] but is not further investigated here for brevity. Note that this model is also valid for positive applied pressures, that is, the pressure is applied to the outside rather than a vacuum applied to the inside of the drum, in which case pressures greater than atmospheric can be used.

The particle flux at the membrane is zero such that, from Eqs. 7, 10, and 14, the concentration gradient at the membrane is:

$$\left.\frac{\partial \phi}{\partial z}\right|_0 = -s \frac{\phi_\infty}{D_\infty} \tag{15}$$

D_∞ is $D(\phi_\infty)$.

An exact similarity solution exists for this problem, analogous to cake formation in the dead-end filtration case,[20] which is an important result showing that the parabolic rule for filtration below the gel point holds for compressible as well as incompressible materials, regardless of the constitutive equation used to describe the network strength or liquid drag. The similarity variable, X, takes the form:

$$X(z,t) = \frac{z}{z_c(t)} \tag{16}$$

such that

$$\phi(z,t) = \left\{ \begin{array}{ll} \Phi(X) & z \le z_c(t) \\ \phi_0 & z > z_c(t) \end{array} \right\} \tag{17}$$

The similarity solution exists for z_c and s varying with the square-root of t:

$$z_c(t) = \gamma\sqrt{t}$$
$$s(t) = \frac{\alpha}{z_c(t)} \tag{18}$$

Making the change of variables to X in Eq. 9 and substituting Eq. 18 gives an ordinary differential equation for the local concentration as a function of X:

$$\frac{d}{dX}\left(D(\Phi)\frac{d\Phi}{dX}\right) + \left(\frac{\gamma^2}{2}X + \alpha\right)\frac{d\Phi}{dX} = 0 \tag{19}$$

The boundary conditions become:

$$\Phi(0) = \phi_\infty \quad \left.\frac{d\Phi}{dX}\right|_0 = -\alpha\frac{\phi_\infty}{D_\infty}$$
$$\Phi(1) = \phi_g \quad \left.\frac{d\Phi}{dX}\right|_1 = -\left(\alpha + \frac{\gamma^2}{2}\right)\frac{\phi_g - \phi_0}{D_g} \tag{20}$$

The problem is further simplified by changing variables from X to η, defined as:

$$\eta = \left(\alpha + \frac{\gamma^2}{2}\right)(1 - X) \tag{21}$$

The ordinary differential equation (Eq. 19) becomes:

$$\frac{d}{d\eta}\left(D(\Phi)\frac{d\Phi}{d\eta}\right) - \left(1 - \frac{\delta^2}{2}\eta\right)\frac{d\Phi}{d\eta} = 0 \tag{22}$$

where δ is:

$$\delta = \left(\frac{\alpha}{\gamma} + \frac{\gamma}{2}\right)^{-1} \tag{23}$$

The boundary conditions become:

$$\Phi(0) = \phi_g \quad \left.\frac{d\Phi}{d\eta}\right|_0 = \frac{\phi_g - \phi_0}{D_g}$$
$$\Phi(\eta^*) = \phi_\infty \quad \left.\frac{d\Phi}{d\eta}\right|_{\eta^*} = \left(1 - \frac{\delta^2\eta^2}{2}\right)\frac{\phi_\infty}{D_\infty} \tag{24}$$

where η^* is:

$$\eta^* = \alpha + \frac{\gamma^2}{2} \tag{25}$$

A numerical solution is required to allow for any arbitrary functions of $p_y(\phi)$ and $R(\phi)$. For an initial estimate of δ, Eq. 22 is solved using a Runge-Kutta numerical technique[21] from $\eta = 0$ until $\Phi = \phi_\infty$, where $\eta = \eta^*$. δ is iterated using an interval halving method until the gradient at η^* satisfies the fourth boundary condition. α and γ (and therefore z_c and s) are given by rearranging Eqs. 23 and 25:

$$\alpha = \eta^*\left(1 - \frac{\eta^*\delta^2}{2}\right)$$
$$\gamma = \eta^*\delta \tag{26}$$

The average solids concentration when the cake exits the bath, ϕ_F, is given by:

$$\phi_F = \frac{1}{z_{c,F}}\int_0^{z_{c,F}} \phi(z, t_F)dz = \frac{1}{\eta^*}\int_0^{\eta^*} \Phi(\eta)d\eta \tag{27}$$

$z_{c,F}$ is the cake height when the cake exists the bath. The solids throughput, Q, is determined by the amount of cake formed while the drum is submerged:

$$Q = \omega r_d L \int_0^{z_{c,F}} \phi(z, t_F)dz \tag{28}$$

Substituting Eq. 27 and simplifying gives:

$$Q = \sqrt{\omega\theta_F}r_d L\delta\int_0^{\eta^*} \Phi(\eta)d\eta \tag{29}$$

As the similarity solution depends only on the vacuum pressure, the material characteristics and the slurry concentration, ϕ_F is independent of the cake formation time and the throughput varies proportionally with $\sqrt{\omega\theta_F}r_d L$. The conclusion is that the theoretical maximum throughput of a vacuum drum filter is when the drum is completely submerged and rotating as fast as possible.

Cake consolidation

When the drum lifts the cake from the feed slurry, the capillary forces at the surface of the cake cause the cake to consolidate. Cake consolidation is particularly important for very fine materials where the capillary forces are large. The solids pressure at the cake surface, and thus the surface solids concentration, is equal to the capillary pressure, $p_{cap}(t)$:

$$p_s(z_c(t), t) = p_y(\phi(z_c(t), t)) = p_{cap}(t) \tag{27}$$

$p_{cap}(t)$ is given by[22]:

$$p_{cap}(t) = \frac{2\gamma_{LV}}{r_{eff}(t)} \tag{28}$$

where $r_{eff}(t)$ is the effective radius of curvature of liquid/air menisci at the cake surface and γ_{LV} is the liquid–vapor surface tension. Fluid drainage causes $r_{eff}(t)$ to decrease and $\phi(z_c(t),t)$ to increase. $p_{cap}(t)$ increases until it equals the maximum capillary pressure, which is given by the Laplace-White equation (developed using thermodynamic arguments of wetting[10]):

$$p_{cap}^{max}(\phi) = \gamma_{LV}\cos\Theta\rho_s\overline{A_s}\frac{\phi}{1 - \phi} \tag{29}$$

where Θ is the receding solid–liquid contact angle, ρ_s is the solids density and $\overline{A}_s$ is the solids specific surface area (m^2/kg). The derivation of Eq. 29 is valid for any internal topology,

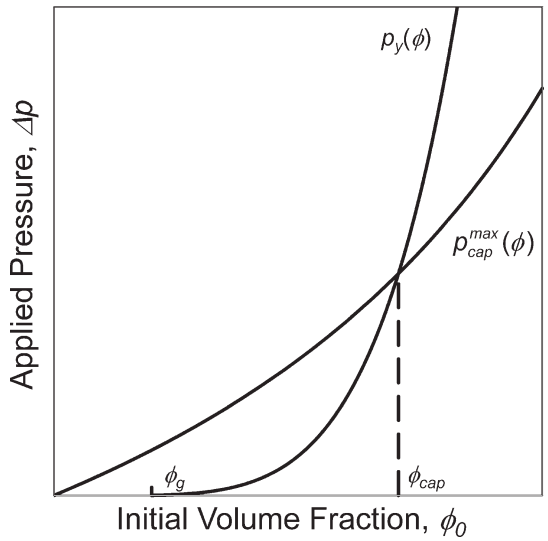

Figure 3. Compressive yield stress, $p_y(\phi)$, and maximum capillary pressure, $p_{cap}^{max}(\phi)$ as functions of solids volume fraction, ϕ.

provided that the network is uniformly packed in the horizontal direction over the length scale of the particles.

$p_y(\phi)$ is generally described by a power-law function of ϕ with a high index, whereas $p_{cap}^{max}(\phi)$ is of the order of ϕ (see Figure 3). The two functions intercept at ϕ_{cap}, which is a critical material property that determines whether a cake will consolidate or desaturate. Below ϕ_{cap}, the pressure required to desaturate the particle network exceeds the network strength and the cake preferentially consolidates rather than desaturates. The cake remains saturated until $\phi(z_c(t),t) = \phi_{cap}$.

During consolidation, the velocity at the top of the cake equals the bulk flow as the overall volume is conserved:

$$\frac{dz_c}{dt} = -s(t) \tag{30}$$

Likewise, the solids velocity at the top of the cake equals the liquid velocity, such that the boundary condition at $z_c(t)$ is:

$$\left.\frac{\partial \phi}{\partial z}\right|_{z_c(t)} = 0 \tag{31}$$

The conservation of solids is given by ϕ_F and $z_{c,F}$:

$$\int_0^{z_c} \phi(z,t)dz = \int_0^{z_{c,F}} \phi(z,t_F)dz = \phi_F z_{c,F} \tag{32}$$

The governing equations for cake consolidation require a numerical solution. Using a backward difference approximation in time, Δt, the coupled first-order ordinary differential equations are:

$$\frac{d\phi}{dz} = \frac{\phi}{D(\phi)}(u_s - s) \tag{33}$$

$$\frac{d(\phi u_s)}{dz} = \frac{\phi - \phi^<}{\Delta t} \tag{34}$$

$$\frac{dI_\phi}{dz} = \phi \tag{35}$$

$\phi^<$ is the value of ϕ at the same z value at the previous time step and I_ϕ is the cumulative solids volume fraction. The volume fraction distribution during cake consolidation is given at progressive steps of s (chosen as 0.01 $s(t_F)$) by solving Eqs. 33 to 35 using a Runge-Kutta numerical technique[21] from the membrane (where $\phi = \phi_\infty$ and $u_s = I_\phi = 0$) to the top of the cake for successive estimates of Δt until the conservation of solids (Eq. 32) is satisfied. For given values of s and Δt, z_c is given by the trapezium rule:

$$z_c = z_c^< - \frac{\Delta t}{2}(s^< + s) \tag{36}$$

$z_c^<$ and $s^<$ are the values of z_c and s at the previous time step. The accuracy of the numerical technique is indicated by the volume fraction gradient at z_c (Eq. 31)

If $\phi_\infty > \phi_{cap}$ (that is, $\Delta p > p_y(\phi_{cap})$), the cake consolidates until, at time t_C, $\phi(z_c,t_C) = \phi_{cap}$ and the cake begins to drain (if the solution at t gives $\phi(z_c,t) > \phi_{cap}$, the step in s is halved until $\phi(z_c,t_C) \approx \phi_{cap}$ to within a user defined accuracy). If $\phi_\infty \le \phi_{cap}$ (that is, $\Delta p \le p_y(\phi_{cap})$, which is especially the case for very fine materials), the cake consolidates until it reaches the knife at $t = t_k$.

Cake desaturation

Beyond t_C if $\Delta p > p_y(\phi_{cap})$, the cake desaturates as the applied pressure at the air–liquid interface, $z_f(t)$, exceeds the maximum capillary pressure of the material and the capillary pressure is less than $p_y(\phi)$. Some fluid is retained in the necks between particles, the residual moisture content of the cake as the liquid front recedes through the porous solid phase, S_e, is the ratio of the liquid volume to the total void volume. S_e is a function of the pressure at which the solid desaturates and is therefore a material property that is a function of ϕ. This description of cake desaturation ignores the effects of cracking and evaporation.

Assuming that the membrane resistance and gravity are insignificant, the solids are immobile during desaturation, such that u_s is zero and the volume fraction distribution and cake height remain at $\phi_C(z) = \phi(z,t_C)$ and $z_c(t_C) = z_{c,C}$, respectively. The rate of filtration is determined from the solids pressure gradient and the liquid volume. The conservation of liquid volume is:

$$\int_0^{z_{c,C}} (1-\phi_C)dz = v(t) - v_C + \int_0^{z_f(t)} (1-\phi_C)dz + \int_{z_f(t)}^{z_{c,C}} S_e(\phi_C)(1-\phi_C)dz \tag{37}$$

where v_C is the filtrate volume at t_C. Differentiating Eq. 37 with respect to t and rearranging gives:

$$\frac{dz_f}{dt} = -\frac{s}{(1-\phi_C(z_f))(1-S_e(\phi_C(z_f)))} \tag{38}$$

With $u_s = 0$, the solids pressure gradient (Eq. 7) is a version of Darcy's law:

$$\frac{\partial p_s}{\partial z} = -\phi_C R(\phi_C) s \tag{39}$$

Integrating Eq. 39 with respect to z from $p_s(0) = \Delta p$ to $p_s(z_f) = p_{cap}^{max}(\phi_C(z_f))$ and rearranging gives:

$$s = \frac{\Delta p - p_{cap}^{max}(\phi_C(z_f))}{I_R(z_f)} \tag{40}$$

where $I_R(z) = \int_0^z \phi_C R(\phi_C) dz$. Substituting dz_f/dt for s from Eq. 38 gives:

$$\frac{dz_f}{dt} = -\frac{\Delta p - p_{cap}^{max}(\phi_C(z_f))}{(1-\phi_C(z_f))(1-S_e(\phi_C(z_f)))I_R(z_f)} \tag{41}$$

Equation 41 is solved using a Runge-Kutta numerical method[21] in steps of Δt (or Δz_f) from $z_f(t_C) = h_C$ until $z_f(t_D) = 0$ (or $t = t_k$).

The magnitude of dz_f/dt increases with time as the hydraulic resistance decreases as more fluid is displaced and approaches $-\infty$ as $z_f \to 0$ as $I_R \to 0$. Neglecting cracking, z_f will always go to 0 if desaturation occurs as $\Delta p > p_{cap}^{max}(\phi_\infty)$ (as long as the combined formation, consolidation and drainage angles are less than $2\pi - \theta_k$).

An important issue during drainage is that the solids volume fraction distribution remains constant at $\phi(z,t_C)$, but the apparent volume fraction, ϕ_{app} (the volume of solids as a fraction of the volume of solids and liquid, effectively the gravimetric solids fraction) increases. The overall volume of the cake is constant, but the moisture content reduces.

Vacuum disc filter model

Figure 2 shows a schematic of a vacuum disc filter, in which the disc is divided into N concentric annuli of width Δr. The vacuum disc filter model uses the same formulations for cake formation, consolidation, and drainage as the drum filter model, with the dewatering equations applied to each annulus. The mid-point radius of the nth annulus is $r_{d,n}$, and the angles of cake formation, consolidation, drainage, and knife position for each annulus are $\theta_{F,n}$, $\theta_{C,n}$, $\theta_{D,n}$, and $\theta_{k,n}$, respectively.

Δr is equal to the submerged depth divided by N. By geometric arguments, Δr is related to the disc radius r_d and the subtended angle θ_F by:

$$\Delta r = \frac{r_d}{N}\left(1 - \cos\left(\frac{\theta_F}{2}\right)\right) \tag{42}$$

If $n = 1$ is the outermost annulus and $n = N$ is the innermost annulus, the mid-point radius of the nth annulus, $r_{d,n}$, is:

$$r_{d,n} = r_d - \Delta r\left(n - \frac{1}{2}\right) \tag{43}$$

The cake formation angle for each annulus, $\theta_{F,n}$, is:

$$\cos\left(\frac{\theta_{F,n}}{2}\right) = \frac{r_d}{r_{d,n}}\cos\left(\frac{\theta_F}{2}\right) \tag{44}$$

The cake formation time for each annulus, $t_{F,n}$, is given by $\theta_{F,n}$ and ω (see Eq. 1). The similarity solution, $\Phi(\eta)$, is independent of $t_{F,n}$ and therefore only needs to be solved once (rather than for each annulus) for the given material properties, operating pressure, and slurry concentration.

The solids throughput for each disc face is derived from the throughput of each annulus in the limit where N goes to infinity:

$$Q = \sqrt{2\omega}\delta\left(\int_0^{\eta^*}\Phi(\eta)d\eta\right)\int_{r_d\cos\frac{\theta_F}{2}}^{r_d} r\sqrt{\cos^{-1}\left(\frac{r_d}{r}\cos\frac{\theta_F}{2}\right)}dr \tag{45}$$

The second integral in Eq. 45 is solved using numerical techniques such as the trapezoidal rule or Simpson's rule. Note that a two-faced disc has a total solids throughput of $2Q$ and a bank of M two-faced discs has a total solids throughput of $2MQ$.

As with the drum filter model, $\phi_{F,n}$ is independent of the cake formation time and the throughput varies proportionally with $\sqrt{\omega}$, such that the maximum throughput is when the disc is rotating as fast as possible. The variation of Q with r_d and θ_F is shown in the results and discussion section.

Materials and Methods

A program was written in Mathematica® to solve the problem as outlined in the formulations above. Arbitrary material properties for $p_y(\phi)$, $R(\phi)$, $p_{cap}^{max}(\phi)$, and $S_e(\phi)$ were used for the purpose of illustrating the model formulation:

$$p_y(\phi) = 100\left[\left(\frac{\phi}{\phi_g}\right)^5 - 1\right]\text{Pa}, \quad \text{where } \phi_g = 0.15\ \text{v/v} \tag{46}$$

$$R(\phi) = 10^8(1-\phi)^{-5.5}\ \text{Pa s/m}^2 \tag{47}$$

$$p_{cap}^{max}(\phi) = 7500\frac{\phi}{1-\phi}\ \text{Pa} \tag{48}$$

$$S_e(\phi) = 0 \tag{49}$$

For these properties, $\phi_{cap} = 0.3029$ v/v and $p_y(\phi_{cap}) = 3259$ Pa. The vacuum drum and disc models were used to give predictions for different operating parameters of θ_F, ω, Δp, and ϕ_0. The drum/disc dimensions were the same in all the simulations ($r_d = 0.5$ m and, for the drum filter, $L = 1$ m).

Results and Discussion

Vacuum drum filter

To illustrate the full solution of the numerical model, the volume fraction distribution and height vs. time results for

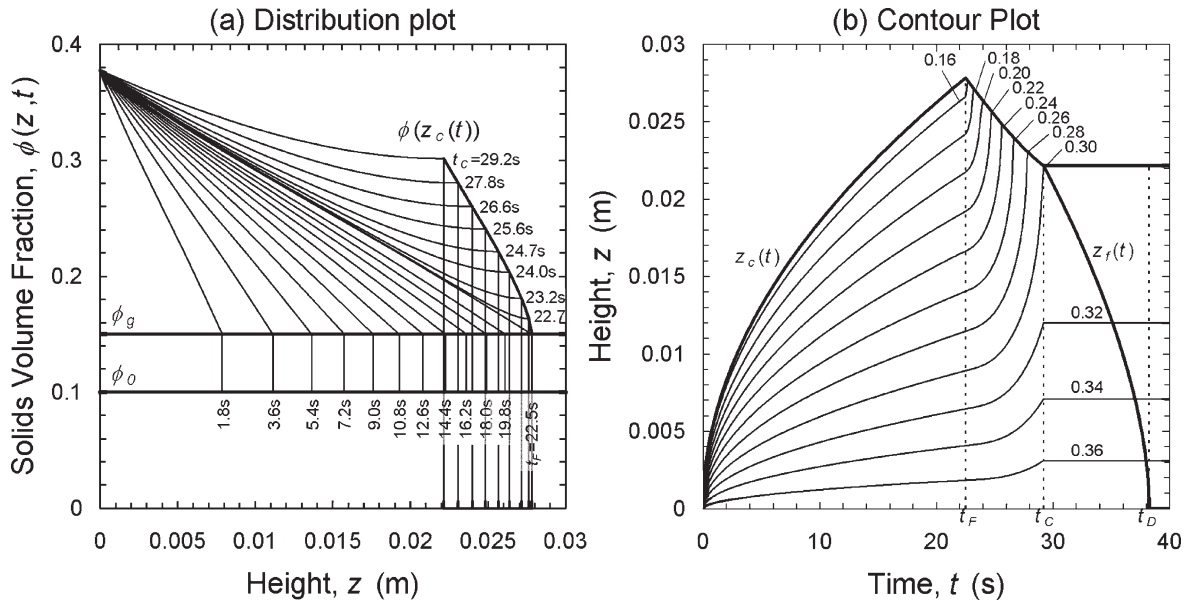

Figure 4. Vacuum drum filter modeling results (a) distribution plot; (b) contour plot (θ_F = 3π/4 rad, ω = π/30 rad/s, Δp = 10 kPa, and ϕ_o = 0.1 v/v).

$\theta_F = 3\pi/4$ rad, $\omega = \pi/30$ rad/s (1 rpm), $\Delta p = 10$ kPa, and $\phi_0 = 0.1$ v/v are presented in Figure 4. At this pressure, $\phi_\infty = 0.3775$ v/v. The results show the build-up of cake on the membrane during cake formation. The volume fraction is ϕ_∞ at the membrane, ϕ_g at the top of the cake, and ϕ_0 in the slurry bath. Cake formation proceeds until $t_F = 22.5$ s. Beyond t_F, the cake consolidates with the concentration at the top of the cake increasing from ϕ_g to ϕ_{cap} at $t_C = 29.2$ s. $d\phi/dz$ approaches 0 at z_c. After t_C, the liquid front recedes into the immobile solids until $t_D = 38.2$ s.

The vacuum drum model was used to investigate the effect of varying the operating parameters. The results for the various angles of consolidation and drainage (θ_C and θ_D, respectively) with angular velocity, ω, at $\theta_F = \pi/2$ rad, $\Delta p = 10$ kPa, and $\phi_0 = 0.1$ v/v are presented in Figure 5. The results indicate that θ_C and θ_D for a given θ_F are independent of ω, which is an important consequence of the similarity solution for cake formation. The cake height is inversely proportional to the square-root of ω (as t_F is inversely proportionally with ω), but so are the consolidation and drainage times (as the rates are all governed by the same material property, the solid–liquid drag), such that angles remain constant. As Q increases with ω, the drum should be operated at maximum speed because it will not affect the quality of the cake. Note that the drainage time was derived assuming no cracking or percolation through the desaturated network which may introduce other rate-determining factors such that θ_D may be a function of ω. In this case, the above conclusion will not hold when $\Delta p > p_y(\phi_{cap})$ (that is, for coarse materials) or $\theta_F + \theta_C < 2\pi - \theta_k$.

The operator of a rotary filter plant can have the option of setting the depth of the slurry bath or equivalently the height of the drum. Figure 6 shows the drum filter results for the variation of θ_C and θ_D with θ_F. θ_C and θ_D vary linearly with θ_F until the knife comes into effect (in this case, $\theta_k = 0$ such that the knife is at the surface of the slurry bath). The linear variation stems from the same reason as the independence of θ_C and θ_D with ω. The combined formation, consolidation, and drainage angles must be less than or equal to $2\pi - \theta_k$ rads, such that θ_D begins to fall once θ_F and θ_C are greater than $2\pi - \theta_D - \theta_k$ rads (at $\theta_F = 3.71$ rad). Likewise, once $\theta_D = 0$ (at $\theta_F = 4.86$ rad), θ_C also begins to decrease.

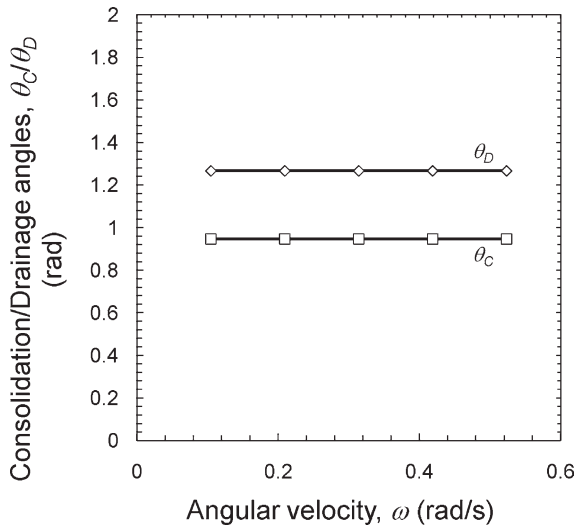

Figure 5. Vacuum drum filter modeling results of consolidation and drainage angles as functions of angular velocity (θ_F = π/2 rad, Δp = 10 kPa, and ϕ_o = 0.1 v/v).

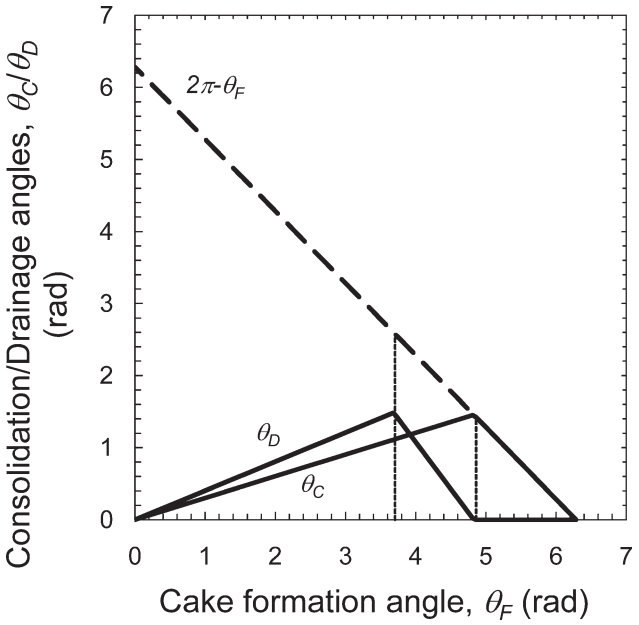

Figure 6. Vacuum drum filter modeling results of consolidation and drainage angles as functions of cake formation angle (ω = π/30 rad/s, Δp = 10 kPa, ϕ_0 = 0.1 v/v, and θ_k = 0).

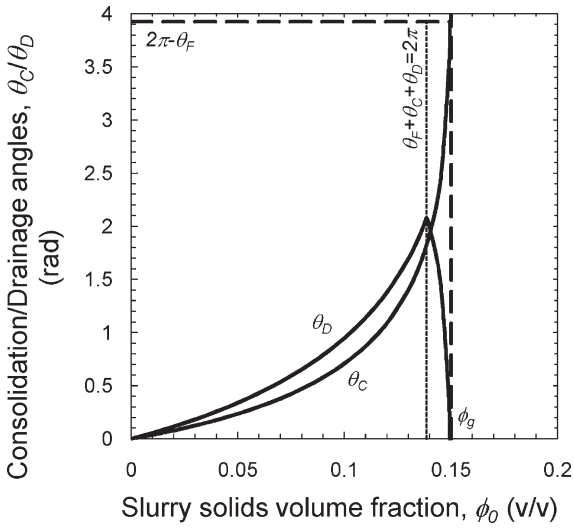

Figure 8. Vacuum drum filter modeling results of consolidation and drainage angles as functions of slurry solids volume fraction (θ_F = 3π/4 rad, ω = π/30 rad/s, Δp = 10 kPa, and θ_k = 0).

The effect of the variation of θ_F on Q, ϕ_C, and ϕ_{app} is shown in Figure 7. Q varies with the square-root of θ_F. For θ_F greater than 4.86 rad, the cake is saturated (that is, θ_D = 0) and the average volume fraction reduces with increasing θ_F as there is less time for consolidation. Below this value, θ_C is constant, therefore ϕ_C is constant. For $3.71 < \theta_F < 4.86$, ϕ_{app} varies between ϕ_C and 1 due to incomplete drainage. As S_e is set to 0, ϕ_{app} goes to 1 as all the liquid is drained from the cake. This value of S_e is not realistic as there will be some liquid retained in the cake, but it illustrates the important difference between volume and weight fraction for desaturated cakes. The optimum slurry depth for the lowest cake moisture content at the highest throughput is when θ_D is greatest ($\theta_F + \theta_C + \theta_D + \theta_k = 2\pi$ rads); θ_F = 3.71 rads in this case.

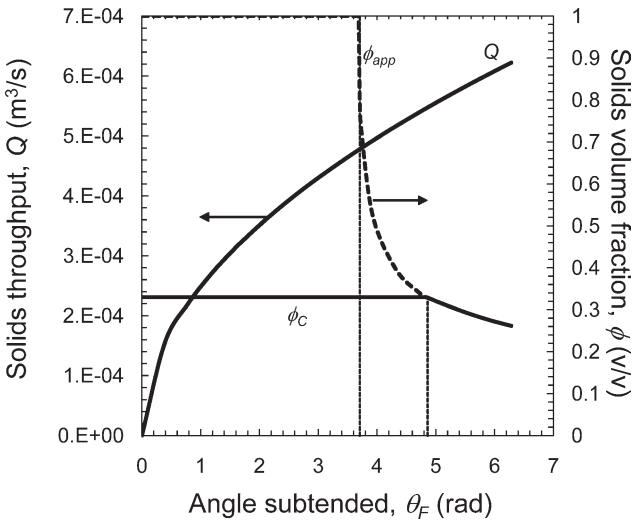

Figure 7. Vacuum drum filter modeling results of solids throughput (Q) and average (ϕ_C) and apparent (ϕ_{app}) solids volume fraction as functions of angle subtended (ω = π/30 rad/s, Δp = 10 kPa, ϕ_0 = 0.1 v/v, and θ_k = 0).

The feed solids to the filter will naturally vary in any operation. The variation of the consolidation and drainage angles with ϕ_0 varying from 0 to ϕ_g is shown in Figure 8. θ_C and θ_D increase with ϕ_0 at a given θ_F since more cake is formed. θ_D increases until $\theta_C + \theta_D = 2\pi - \theta_F - \theta_k$ (ϕ_0 = 0.1385 v/v), beyond which incomplete drainage is seen. θ_C continues to rise until equal to $2\pi - \theta_F - \theta_k$, which, in this case, is close to ϕ_g. θ_C and θ_D begin to asymptote as $\phi_0 \rightarrow \phi_g$ due to the assumption that all networked material is in the cake that is lifted out of the bath. Consequently, when $\phi_0 = \phi_g$, all of the slurry in the bath is in the cake.

Figure 9 shows Q as a function of ϕ_0 for three pressures. Q grows monotonically with ϕ_0. The conclusion is that the best operating condition is when ϕ_0 is highest, allowing for geometrical considerations to allow for complete drainage. Q asymptotes to infinity as $\phi_0 \rightarrow \phi_g$ due to the assumption that all material above the gel point is in the cake. The pressure variation of Q in Figure 9 allows quantification of the possible improvement in throughput by raising the vacuum pressure against the cost of the additional pressure. For example, increasing the vacuum pressure from 5 to 20 kPa at $\phi_0 = 0.1$ v/v increases the throughput by 28%.

The results for the variation of the consolidation and drainage angles with pressure are shown in Figure 10. For vacuum pressures below $p_y(\phi_{cap})$ = 3259 Pa, there is no drainage because the pressure is insufficient to overcome the capillary pressure at the top of the cake. This is an important result for very fine materials where p_{cap}^{max} (ϕ) is large. For pressures greater than $p_y(\phi_{cap})$, the drainage angle is not

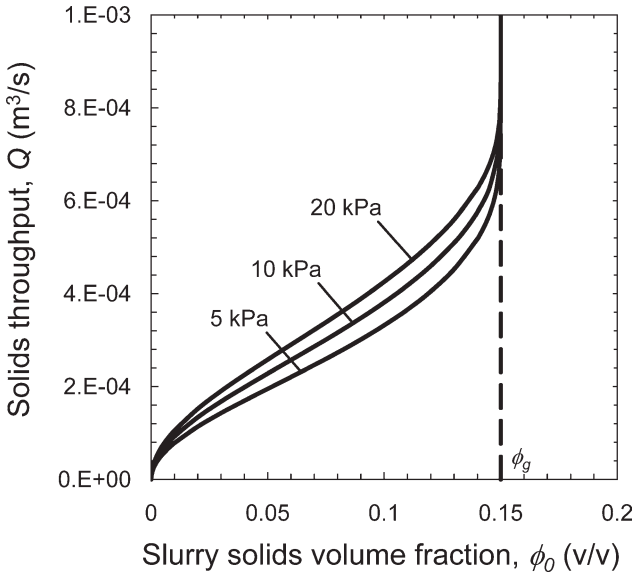

Figure 9. Vacuum drum filter modeling results of solids throughput as a function of slurry solids volume fraction ($\theta_F = 3\pi/4$ rad, $\omega = \pi/30$ rad/s, $\Delta p = 10$, 5 and 20 kPa, and $\theta_k = 0$).

zero, and the sum of θ_C and θ_D is $2\pi - \theta_F$. Above a certain pressure (4680 Pa in this case), the cake completely drains before reaching the knife.

Vacuum disc filter

A schematic of the predictions of the vacuum disc filter model is shown in Figure 11. The angles of cake consolidation and drainage vary proportionally with the angle of cake formation, such that the degree of dewatering varies with radius. The outermost annulus requires the most distance, whereas the innermost annulus requires very little consolidation and drainage time. To reduce the chance of cake cracking, the knife edge should be a function of radius. In the limit where Δr goes to zero, material at the surface of the slurry bath ($r = r_d\cos(\theta_F/2)$) is infinitely thin and the volume fraction is at ϕ_g. θ_C and θ_D at this radius are zero. The consequence of this is to either have the knife at the slurry surface at $\theta_F/2$, or to incorporate a nonfiltering disc that is partly submerged, eliminating the inner annuli.

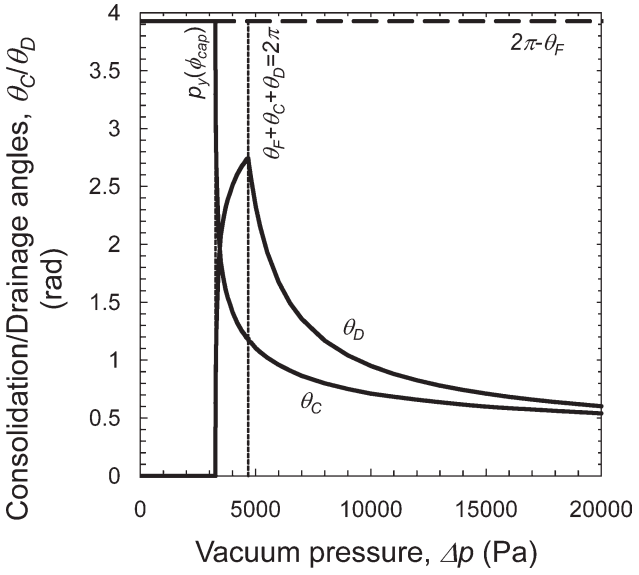

Figure 10. Vacuum drum filter modeling results of consolidation and drainage angles as functions of applied pressure ($\theta_F = 3\pi/4$ rad, $\omega = \pi/30$ rad/s, $\phi_0 = 0.1$ v/v, and $\theta_k = 0$).

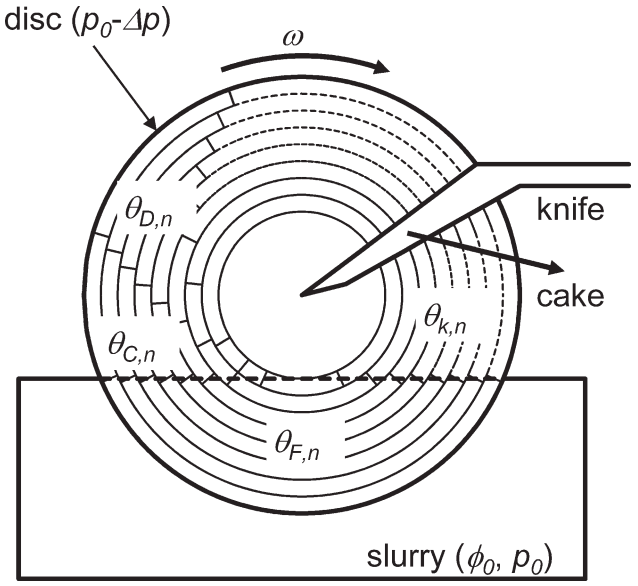

Figure 11. Schematic of vacuum disc filter divided into eight segments, showing cake formation, consolidation and drainage for each segment ($N = 8$, $\theta_F = 3\pi/4$ rad, $\Delta p = 10$ kPa, and $\phi_0 = 0.1$ v/v).

The arbitrary decision of the number of annuli affects the accuracy of the cake profile. $z_{c,F}$ varies with the square-root of time as shown by the similarity solution (see Eq. 18) and is therefore related to the radius through Eqs. 1 and 44. The error in the approximation falls progressively with higher values of N: in the example used here, the throughput for $N = 2$ is within 1.0% of the true value; for $N = 16$, the throughput is within 0.10%, and for $N = 32$, it is within 0.05%. Obviously, using more annuli improves the accuracy but more computing time is required.

The throughput of a disc filter is given by Eq. 45, which states explicitly that Q varies proportionally with $\sqrt{\omega}$. The integral component on the right-hand side of Eq. 45 has been evaluated numerically for a range of r_d and θ_F values, and the results shown in Figure 12. The throughput varies exactly with r_d^2, which is expected as the cake forms on the area of the disc. In comparison, Q varies linearly with r_d for the drum filter as the cake forms on the circumference. Q increases monotonically with θ_F (although not with $\sqrt{\theta_F}$ as for the drum filter), such that the maximum throughput of a vacuum disc filter is when the disc is half submerged ($\theta_F = \pi$). $\theta_F = \pi$ is the maximum subtended angle as greater angles would result in material never emerging from the slurry bath.

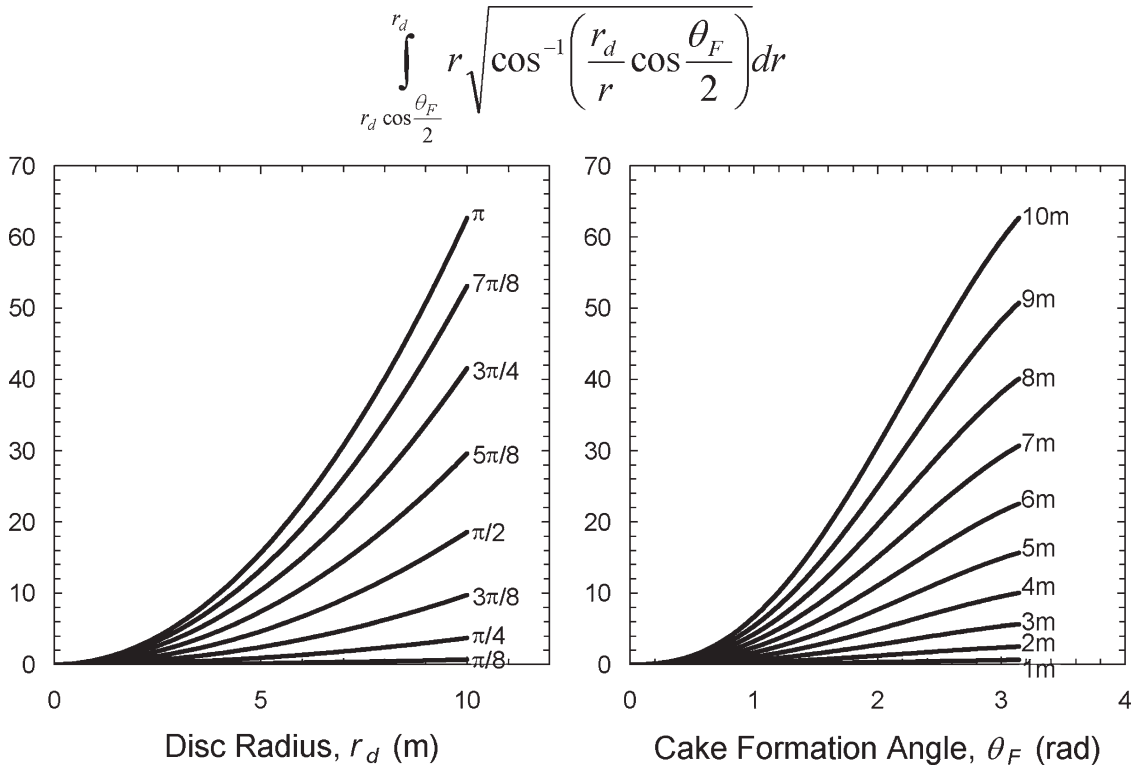

Figure 12. Integral component of solids throughput, *Q* (see Eq. 45), as a function of the disc radius, r_d, and the angle subtended, θ_F, for a disc filter.

Conclusions

This work details the formulation of models for rotary vacuum drum and disc filters using compressional rheology theory. The conservation of mass and momentum equations are given in one-dimension and rearranged to give the governing equation for pressure filtration. The initial and boundary conditions for cake formation, consolidation, and drainage are outlined and used to give solutions for each process. The disc filter model uses the drum filter formulation applied to concentric annuli.

Assuming that the membrane resistance and the hydrostatic pressure are insignificant, an exact similarity solution exists for cake formation (analogous to dead-end filtration) in which the cake height and filtrate volume vary with the square-root of time. A consequence of the similarity solution is that the drum filter throughput varies with $\sqrt{\omega\theta_F}r_d L$, and the disc filter throughput varies with $\sqrt{\omega}r_d^2$ and increases monotonically with θ_F. Once cake is removed from the slurry bath, it undergoes consolidation and drainage. The extent of each process is determined by the $p_y(\phi)$ and $p_{cap}^{max}(\phi)$ material properties—if the yield stress is less than the capillary pressure, the network will preferentially compress rather than desaturate, and vice versa if the capillary pressure is less than the yield stress. A numerical scheme is outlined to solve the governing equations for cake consolidation—this work represents the first description of cake compression in rotary filters. The models are used to give predictions of performance for a range of operating conditions.

Acknowledgments

Two of the authors (A.D.S. and P.J.S.) acknowledge financial support by the Australian Research Council through the Particulate Fluids Processing Centre (a Special Research Centre of the ARC) and an ARC Discovery Grant.

Notation

Roman letters

$\overline{A}_s$ = specific surface area of solids (m^2/kg)
$D(\phi)$ = solids diffusivity (m^2/s)
L = drum length (m)
I_ϕ, I_R = integrals of ϕ and $\phi R(\phi)$
M = number of discs
N = number of concentric annuli for disc model
n = annulus number
p = pressure (Pa)
$p_y(\phi)$ = compressive yield stress (Pa)
$p_{cap}^{max}(\phi)$ = maximum capillary pressure (Pa)
Q = solids throughput (m^3/s)
$R(\phi)$ = hindered settling function (Pas/m^2)
r_d = drum/disc radius (m)
r_{eff} = effective radius of curvature (m)
S_e = residual saturation
s = suspension flux (m/s)
t = time (s)
u = velocity (m/s)
v = specific filtrate volume (m)
X = similarity variable
z = normal coordinate (m)

Greek letters

α = similarity solution constant for $s(t)$ (m^2/s)
δ = similarity solution constant

Δp = vacuum pressure (Pa)
Δt = time step (s)
ϕ, Φ = solids volume fraction (v/v)
γ = similarity solution constant for $z_c(t)$ ($m/s^{1/2}$)
γ_{LV} = liquid–vapor surface tension (N/m)
η = similarity variable (m^2/s)
η^* = similarity solution constant (m^2/s)
θ = angle (rad)
Θ = solid–liquid contact angle (rad)
ρ_s = solids density (kg/m^3)
ω = angular speed (rad/s)

Superscripts/subscripts

$^<$ = value at previous time step
$_0$ = initial
$_{app}$ = apparent
$_c$ = cake
$_{cap}$ = capillary
$_C$ = consolidation
$_D$ = drainage
$_f$ = fluid
$_F$ = formation
$_g$ = gel point
$_k$ = knife
$_l$ = liquid
$_s$ = solid
$_\infty$ = equilibrium

Literature Cited

1. White DA. Prediction of leaching and filtration performance of drum filters. *Chem Eng Sci*. 1976;31:419–425.
2. Nicolaou I, Stahl W. Calculation of rotary filter plants. *Auf-Tech*. 1992;33:328–338.
3. Rushton A. Pressure variation effects in rotary drum filtration with incompressible cakes. *Powder Tech*. 1978;20:39–46.
4. Rushton A. Design throughputs in rotary disc vacuum filtration with incompressible cakes. *Powder Tech*. 1978;21:161–169.
5. Tiller FM, Risbud H. Analytical formulas for disc filters. *AIChE J*. 1974;20:36–42.
6. Buscall R, White LR. The consolidation of concentrated suspensions, Part 1: The theory of sedimentation. *J Chem Soc Faraday Trans I*. 1987;83:873–891.
7. Landman KA, Sirakoff C, White LR. Dewatering of flocculated suspensions by pressure filtration. *Phys Fluids A*. 1991;3:1495–1509.
8. Howells I, Landman KA, Panjkov A, Sirakoff C, White LR. Time dependent batch settling of flocculated suspensions. *Appl Math Model*. 1990;14:77–86.
9. Stickland AD, White LR, Scales PJ. Modeling of solid-bowl batch centrifugation of flocculated suspensions. *AIChE J*. 2006;52:1351–1362.
10. White LR. Capillary rise in powders. *J Colloid Interface Sci*. 1982; 90:536–538.
11. Brown LA, Zukoski CF, White LR. Consolidation during the drying of aggregated suspensions. *AIChE J*. 2002;48:492–502.
12. Brown LA, Zukoski CF. Experimental tests of two-phase fluid model of drying consolidation. *AIChE J*. 2003;49:362–372.
13. Barr JD, White LR. Centrifugal drum filtration. II. A compression rheology model of cake draining. *AIChE J*. 2006;52:557–564.
14. Stickland AD, de Kretser RG, Scales PJ. One-dimensional model of vacuum filtration of compressible flocculated suspensions. *AIChE J*. 2010; Early View (DOI: 10.1002/aic.12194).
15. Baluais G, Dodds JA, Tondeur T. A model for the desaturation of porous media as applied to filter cakes. *Int Chem Eng*. 1985;25:436–446.
16. Wakeman RJ. Low-pressure dewatering kinetics of incompressible filter cakes. II. Constant total pressure loss or high-capacity systems. *Int J Miner Proc*. 1979;5:395–405.
17. Condie DJ, Hinkel M, Veal CJ. Modelling the vacuum filtration of fine coal. *Filt Sep*. 1996;33:825–834.
18. Landman KA, White LR. Solid/liquid separation of flocculated suspensions. *Adv Colloid Interface Sci*. 1994;51:175–246.
19. Landman KA, White LR, Buscall R. The continuous flow gravity thickener: steady state behaviour. *AIChE J*. 1988;34:239–252.
20. Landman KA, White LR. Predicting filtration time and maximizing throughput in a pressure filter. *AIChE J*. 1997;43:3147–3160.
21. Matthews JH. *Numerical Methods for Mathematics, Science, and Engineering*, 2nd ed. New Jersey: Prentice-Hall, 1992.
22. Hunter RJ. *Foundations of Colloid Science*, 2nd ed. Oxford: Oxford University Press, 2001.

Manuscript received Nov. 6, 2009, and revision received Apr. 15, 2010.